



Published in final edited form as:

Proc SPIE. 2012 March 23; 8317: . doi:10.1117/12.916097.

In Vivo Imaging and Quantification of Iron Oxide Nanoparticle Uptake and Biodistribution

P. Jack Hoopes^{a,b}, Alicia A. Petryk^a, Barjor Gimi^b, Andrew J. Giustini^{a,b}, John B. Weaver^{a,b}, John Bischof^{c,d}, Ryan Chamberlain^e, and Michael Garwood^{e,f}

^aThayer School of Engineering at Dartmouth, 8000 Cummings Hall, Hanover, NH, USA 03755

^bDartmouth Medical School (Departments of Surgery, Radiation Oncology and Radiology), 1 Rope Ferry Rd., Hanover, NH, USA 03755

^cDepartment of Mechanical Engineering, University of Minnesota, 111 Church St. SE, Minneapolis, MN, USA 55455

^dDepartment of Biomedical Engineering, University of Minnesota, 312 Church St. SE, Minneapolis, MN, USA 55455

^eCenter for Magnetic Resonance Research, University of Minnesota, 2021 Sixth St. SE, Minneapolis, MN, USA 55455

^fDepartment of Radiology, University of Minnesota, 420 Delaware St. SE, Minneapolis, MN, USA 55455

Abstract

Recent advances in nanotechnology have allowed for the effective use of iron oxide nanoparticles (IONPs) for cancer imaging and therapy. When activated by an alternating magnetic field (AMF), intra-tumoral IONPs have been effective at controlling tumor growth in rodent models. To accurately plan and assess IONP-based therapies in clinical patients, noninvasive and quantitative imaging technique for the assessment of IONP uptake and biodistribution will be necessary.

Proven techniques such as confocal, light and electron microscopy, histochemical iron staining, ICP-MS, fluorescent labeled mNPs and magnetic spectroscopy of Brownian motion (MSB), are being used to assess and quantify IONPs *in vitro* and in *ex vivo* tissues. However, a proven noninvasive *in vivo* IONP imaging technique has not yet been developed. In this study we have demonstrated the shortcomings of computed tomography (CT) and magnetic resonance imaging (MRI) for effectively observing and quantifying iron/IONP concentrations in the clinical setting. Despite the poor outcomes of CT and standard MR sequences in the therapeutic concentration range, ultra-short T2 MRI methods such as, *Sweep Imaging With Fourier Transformation* (SWIFT), provide a positive iron contrast enhancement and a reduced signal to noise ratio. Ongoing software development and phantom and *in vivo* studies, will further optimize this technique, providing accurate, clinically-relevant IONP biodistribution information.

Keywords

iron oxide; magnetic nanoparticle; hyperthermia; MRI; SWIFT

1) INTRODUCTION

The development of iron oxide nanoparticles for hyperthermia applications has great potential for delivering focused and effective cell killing. Previous hyperthermia methods were hindered by the difficulties of low tumor specificity and the delivery of a quantifiable and repeatable thermal dose to the targeted tissue while avoiding normal tissue toxicity. Because of the localized nature of delivery mechanism (the heat sources are within the cells) and the promise of future specificity via protein/antibody targeting, the technology has great potential. The IONP used by our group, for IONP hyperthermia (IONPHT), are Fe₃O₄ cores with a biocompatible hydroxyethyl starch coating (Micromod Partikeltechnologie GmbH (18119 Rostock-Warnemuende, GERMANY)). When an alternating magnetic field is applied (170 kHz and 400–600 Oe) the particles heat via hysteresis, with significant tumor regrowth delay demonstrated *in vitro*, in murine breast cancer models and spontaneous oral canine tumors, both alone and with adjuvant radiation and chemotherapy^{1, 2, 3,4}

The ability to accurately measure the *in vivo* distribution of IONP is essential to develop IONPHT into a clinical cancer treatment. Through our own efforts (Dartmouth and University of Minnesota), we have determined that standard MR imaging techniques are unable to visualize concentrations greater than 1mg Fe/g tissue, which studies suggest have the greatest potential to generate significant efficacy. Zhou et al. identified the two primary problems associated with imaging IONP with GRE sequences as: 1) The signal void created by the IONP is larger than the cells containing them, which in bulk tissues is manifested by large “holes” in the image, 2) Signal voids are difficult to distinguish from other sources of T2* shortening, such as the tissue/air boundaries. This results in a negative contrast, with both poor signal-to-noise ratios and specificity.⁵ CT imaging is also inadequate as it lacks the sensitivity necessary at the concentrations applied. Although CT is used clinically for measuring IONP, at concentrations at 10 mg Fe/mL tissue and below, the degree of contrast-concentration resolution significantly drops off.⁶ Other methods of imaging and quantification such as TEM, histology techniques, and ICP-MS lack the ability to measure IONP levels in living tissue. Furthermore, although they have many applications in experimental settings, fluorescence methods are impractical in the clinic. The presented data and images demonstrate the aforementioned shortcomings of the standard techniques as well as propose a promising solution in the form of the *Sweep Imaging With Fourier Transformation* (SWIFT) MR method.

2) METHODOLOGY

2.1 Iron Oxide Nanoparticles

BNF-IONPs consist of a magnetite core, coated with biocompatible hydroxyethyl starch (110–120 nm hydrodynamic diameter), acquired from Micromod Partikeltechnologie GmbH (18119 Rostock-Warnemuende, GERMANY).

2.2 Mouse Tumor Models

An MTGB mouse mammary adenocarcinoma was grown in the flanks of female C3H mice (Charles River Laboratories, Wilmington, MA 01887 USA). Tumors were injected

approximately 3 weeks post implantation ($\sim 300 \text{ mm}^3$) with 7.5 mg of Fe (total IONP concentration of 42 mg/mL, containing 28 mg of Fe/mL) per cm^3 of tumor.

2.3 Dog Tumor Model and Treatment

Mircomod BNF IONP (Micromod Partikeltechnologie GmbH (18119 Rostock-Warnemuende, GERMANY)) were injected directly into a spontaneous acanthomatous ameloblastoma and activated 30 minutes later. The coil used to produce the AMF was a pancake coil (Fluxtrol Inc., Auburn Hills, MI), driven by a 25k generator (Precision Power System & Technology Inc. (Watsonville, CA, USA)). The tumor also received 6 fractions of radiation @ 4 Gy each (Figure 1).

2.4 Phantoms

Five tubes containing different concentrations of IONP (Ferrotec (Santa Clara, CA 95054 USA) EMG-308; diameter $\sim 10 \text{ nm}$) in 1% agarose gel, placed in a beaker of pure saline, were used as MRI imaging phantoms

2.5 MRI

in vivo spin echo MRI images were acquired using a 9.4 T Varian MRI (Varian Medical Systems Inc (Palo Alto, CA 94304 USA)).

Mouse 1: Repetition time TR = 1000 ms, echo time TE = 14.52 ms field-of-view = $60 \times 60 \text{ mm}$, acquisition matrix = 128×128 , 10 slices, slice thickness = 2mm, one signal average (Figure 2).

Mouse 2: T1 images were acquired with: repetition time TR = 700 ms, echo time TE = 16.38 ms field-of-view = $40 \times 40 \text{ mm}$, acquisition matrix = 256×256 , 10 slices, slice thickness = 2mm, one signal average. T2 images were acquired with: repetition time TR = 1500 ms, echo time TE = 40 ms field-of-view = $40 \times 40 \text{ mm}$, acquisition matrix = 256×256 , 10 slices, slice thickness = 2mm, one signal average (Figure 3).

Dog: Three weeks following the initial IONP injection and IONPHT treatment, an MRI was taken of the dog on a 3T Philips MRI (Philips Electronics North America Corporation (Andover, MA 01810 USA)). Images were acquired using a T1 FFE/GR sequence with the following acquisition parameters: repetition time TR = 550 ms, echo time TE = 2 ms, field-of-view FOV = 200 mm, acquisition matrix = 512×512 , 54 slices, slice thickness = 2 mm (Figure 6).

Phantoms: Images were acquired with GRE, SE, and SWIFT sequences (Figure 9). We created a phantom composed of five NMR tubes with commercially available IONP (Ferrotec (Santa Clara, CA 95054 USA) with concentrations ranging from 0.01–1.0 mg Fe/ml in 1% agarose gel. They were immersed in distilled water and imaged with a volume coil at 9.4 T. After the AHP saturation pulse, 4096 SWIFT projections were acquired using SWIFT with TR = 1 ms; flip = 5° ; bandwidth = 104 kHz. GRE (echo time = 2.5 ms) and SE (echo time = 16.5 ms) (Figure 7).

2.6 CT

microCT images (GE Healthcare, Product Technology-eXplore Locus MicroCT Scanner, Pre-Clinical CT Imaging, Little Chalfont (United Kingdom)) were acquired at 40 kvp, 400 mA, resolution 21 microns, 180 degrees, 1/2 degree apart FOV = 12 × 12 mm (Figure 4).

2.7 Imaging Procedures

All animal experiments were approved by the Dartmouth College Institutional Animal Care and Use Committee (IACUC), in accordance with all federal, institutional and AAALAC (Association for Assessment and Accreditation of Laboratory Animal Care) guidelines.

Mouse 1: The mouse was anesthetized and scanned in the manner described previously. The animal was removed from the MR and injected in the prescribed manner, and then scanned again immediately following injection using the same imaging parameters (Figure 2).

Mouse 2: The mouse was anesthetized and injected in the manner described previously. The mouse was sacrificed 15 minutes following the injection and imaged with the two acquisition parameters described. CT images were also acquired at this time. Following the CT imaging procedures the tumor was excised, photographed, fixed in formaldehyde, processed for histologic iron staining/Prussian Blue (Figure 3, 4, 5).

Dog: A 10 years old female Schnauzer presented with a oral tumor (Acanthomatous Ameloblastoma) associated with the upper left canine tooth. Upon exam, the dog was anesthetized and the tumor and surrounding area were imaged with conventional T1 and T2 MRI pulse sequences (Figure 6).

3) RESULTS

3.1 Mouse 1 Results

The spin echo images of Mouse 1 show the appearance of tumor tissue with and without IONP. The darkening within the tumor tissue demonstrates the significant voids that result from the presence of the IONP.

3.2 Mouse 2 Results

Regions of high IONP contrast can be seen in the images from both the T1 and T2 scans, although differentiation at the highest concentration is impaired due both the resulting negative contrast with which signal decreases with increasing concentration, and to signal voids which are significantly greater than the IONP volume.

Micro-CT images acquired over the same time period were also unable to distinguish different regions of IONP concentration. However, variations in IONP concentration can be seen within the excised tumor tissue (bulk IONP appear black). Histology confirms significant variation of Fe content as well as movement and aggregation.

3.3 Dog Results

As illustrated in the MRI image below, the imaging artifact created by the low number of IONP was significant and made visualization of the tumor impossible with the applied

imaging sequences. Without a suitable imaging method not only will the ability to effectively predict thermal dose be compromised, but the ability to gauge treatment efficacy will be hindered as well.

3.4 Phantom Results

The *Sweep Imaging With Fourier Transformation* MR method (SWIFT) is suited for the imaging of IONP as the time between excitation and signal acquisition is very short.⁷ Unlike with traditional MRI methods, such as gradient-echo or spin-echo, with which IONP appear as negative contrast, IONP are presented as positive contrast which is easier to accurately distinguish from other tissues or the air-tissue boundary, and therefore, accurately quantify.⁵

4) DISCUSSION

In this paper we demonstrate the importance and difficulty of observing and quantifying iron concentrations in the clinically relevant range for cancer therapy. We have shown that conventional CT and MRI techniques are not capable of adequately imaging or quantifying IONPs in tissues and are thus not useful for IONP hyperthermia treatment planning. We believe a new ultra-short T2 MRI technique (SWIFT) has excellent potential in this regard. Our feasibility studies suggest the SWIFT technique can be accurate over the range of iron concentrations utilized in both intra-tumoral and systemic IONP cancer therapy.

A very important IONP associated imaging issue, that is only briefly addressed here, pertains to the IONP cellular uptake mechanism and kinetic variability present in different tumors and normal tissues. These differences have extremely important ramifications with respect IONP magnetic behavior (T1 and SAR values) and therapeutic potential (heating capability). Ongoing studies at Dartmouth have shown that SAR drastically increases when IONPs are aggregated together in a conformation of 200 nm or greater.⁸ This finding is important especially if the MRI signal changes due to aggregation, which will lead to a more quantifiable assessment of nanoparticle behavior and prediction of thermal dose in the clinical settings.

In summary, the establishment of an imaging method capable of accurately observing and quantify the concentration and distribution of both directly and systemically injected IONP is critical for the future clinical application of IONP hyperthermia cancer treatment. Although CT and other MRI methods are able to image IONP at higher or lower concentrations, the SWIFT MRI method is uniquely suited to image concentrations which are relevant for clinical IONPHT applications.

References

1. Giustini AJ, Petryk AA, Hoopes PJ. Comparison of microwave and magnetic nanoparticle hyperthermia radiosensitization in murine breast tumors. *Proc of SPIE: Energy-based Treatment of Tissue and Assessment VI*. 2011; 7901:79010E-1.
2. Petryk AA, Stigliano RV, Giustini AJ, Gottesman RE, Trembly BS, Kaufman PA, Hoopes PJ. Comparison of iron oxide nanoparticle and microwave hyperthermia alone or combined with cisplatin in murine breast tumors. *Proc of SPIE: Energy-based Treatment of Tissue and Assessment VI*. 2011; 7901:790119-1.

3. Petryk AA, Giustini AJ, Ryan P, Strawbridge RA, Hoopes PJ. Iron oxide nanoparticle hyperthermia and chemotherapy cancer treatment. Proc of SPIE: Energy-based Treatment of Tissue and Assessment V. 2009:7181.
4. Cassim SM, Giustini AJ, Petryk AA, Strawbridge RA, Hoopes PJ. Iron Oxide nanoparticle hyperthermia and radiation cancer treatment. Proc of SPIE: Energy-based Treatment of Tissue and Assessment V. :7181.2009
5. Zhou R, Idiyatullin D, Moeller S, Corum C, Zhang H, Qiao H, Zhong J, Garwood M. SWIFT detection of SPIO-labeled stem cells grafted in the myocardium. Magnetic Resonance in Medicine. 2010; 63(5):1154. [PubMed: 20432286]
6. Gneveckow U, Jordan A, Scholz R, Brüß V, Waldöfner N, Ricke J, Feussner A, Hildebrandt B, Rau B, Wust P. Description and characterization of the novel hyperthermia and thermoablation system MFH300F for clinical magnetic fluid hyperthermia. Medical Physics. 2004; 31:1444. [PubMed: 15259647]
7. Corum C, Idiyatullin D, Moeller S, Park J, Garwood M. Introduction to SWIFT (*Sweep Imaging with Fourier Transformation*) for Magnetic Resonance Imaging of Materials. Mater Res Soc Symp Proc. 2007:984.
8. Giustini AJ, Hoopes PJ, Gottesman RE, Petryk AA, Rauwerdink AM. Kinetics and pathogenesis of intracellular magnetic nanoparticle cytotoxicity. Proc, of SPIE: Energy-based Treatment of Tissue and Assessment. 2011:790118–790118-7.



Figure 1.

Left: IONP were injected directly into a spontaneous canine oral tumor. Center: IONP were activated 30 minutes later with an AMF generated by a pancake coil, driven by a 25k generator. Right: Fifteen days later the visible tumor was significantly smaller and less dark than at the time of treatment. IONP are not grossly visible, in the tissue, at this time.

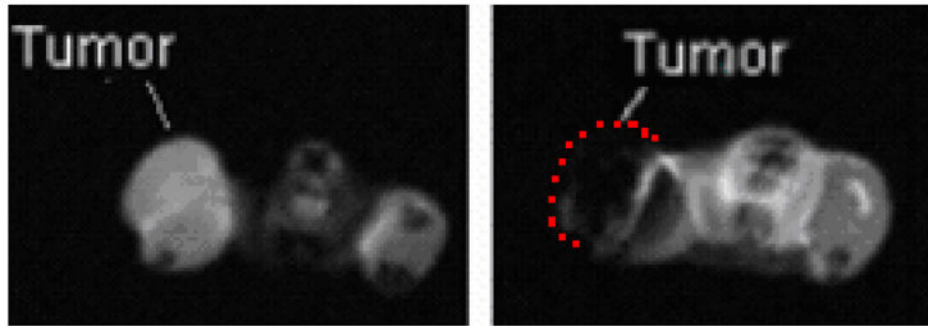


Figure 2.

Left: The initial MRI scan of mouse 1 clearly distinguishes the tumor from the rest of the flank. Right: The scan taken after a direct injection of IONP with 7.5 mg Fe/gram of tumor shows significant quenching of the signal. Tumor location in image at right is indicated by dashed line. Imaging parameters: spin-echo, TR = 1000 ms, TE = 14.52 ms FOV = 60 × 60 mm, acquisition matrix = 128 × 128, 10 slices, slice thickness = 2mm, one signal average.

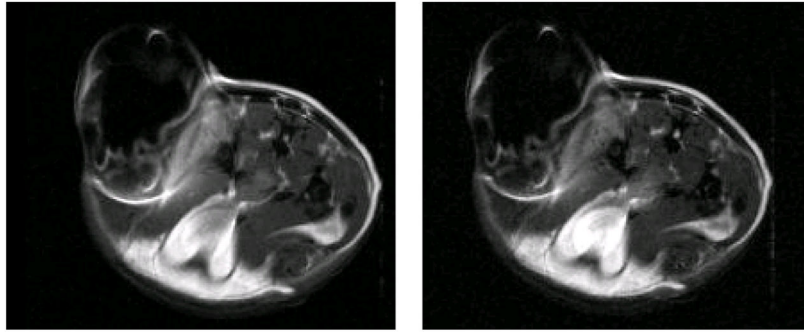


Figure 3.

T1 and T2 spin-echo images of directly injected IONP in the MTGB flank tumor of a female C3H mouse. Right: T1 image, TR = 700 ms, TE = 16.38 ms, FOV = 40×40 mm, acquisition matrix = 256×256 , 10 slices, slice thickness = 2mm, one signal average. Left: T2 image, TR = 1500 ms, TE = 40 ms, FOV = 40×40 mm, acquisition matrix = 256×256 , 10 slices, slice thickness = 2mm, one signal average. In this situation there is little observable difference between the two techniques.

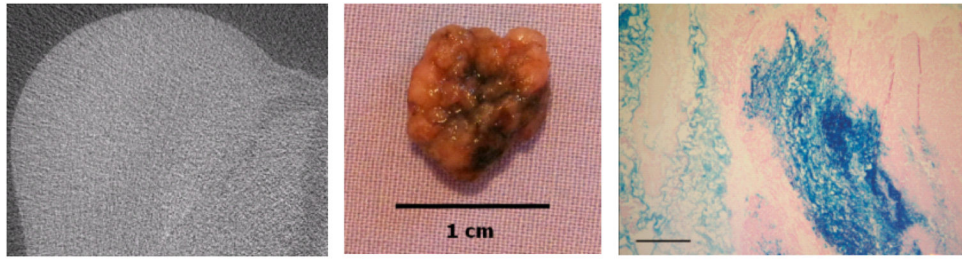


Figure 4.

Left: Micro CT images of directly injected IONP in the MTGB mouse mammary tumor. Slice 504 of 835, 40 kvp, 400 mA, resolution 21 microns, 180 degrees, 1/2 degree apart FOV = 12×12 mm. In general there is very little resolution of either IONPs or tumor tissue. Center: Excised MTGB tumor tissue 15 minutes following IONP injection. IONP are represented by the black staining which can be seen in higher concentrations at the center of the tumor (site of injection). Right: Microscopic section of a murine mammary tumor demonstrating significant aggregation of IONP in central tumor area immediately following a single injection delivery. It should also be notes that some IONPs are rapidly migrating from the injection region. Prussian Blue stain, 15X, scale bar = 1000 microns

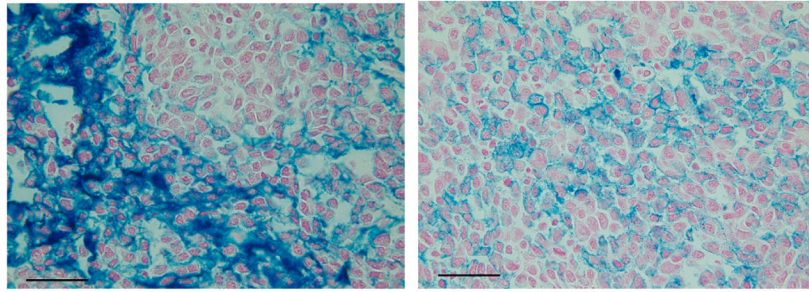


Figure 5. High magnification photomicrographs demonstrating movement and aggregation of IONPs (blue stain) 15 minutes following a single central tumor injection. The photomicrograph on the left demonstrates an area of heavy IONP concentration, while right photomicrograph shows a region of much more evenly distributed IONPs. The fact that the IONPs distribute so well through the tumor and between cells, at such a short incubation time, is encouraging with respect to IONP tumor biodistribution following local tumor injection. Prussian Blue stain, 150X, scale bar =100 microns.

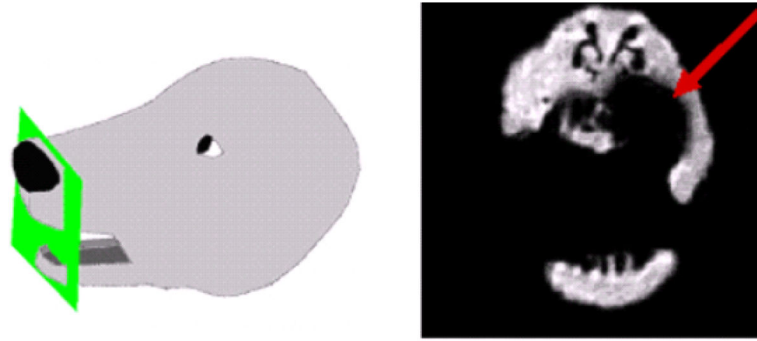


Figure 6.

The diagram on the left demonstrates the location of canine oral tumor and MRI slice. The MRI slice (right image) of the tumor 15 days post injection/treatment demonstrates a void that completely obscures the tumor. The SWIFT-MRI imaging technique has the potential to address this issue, resulting in a positive IONP contrast situation. MRI technique use in the figure above: T1 FFE/GR sequence repetition time TR = 550 ms, echo time TE = 2 ms, FOV= 200 mm, acquisition matrix = 512×512 , 54 slice thickness = 2 mm.

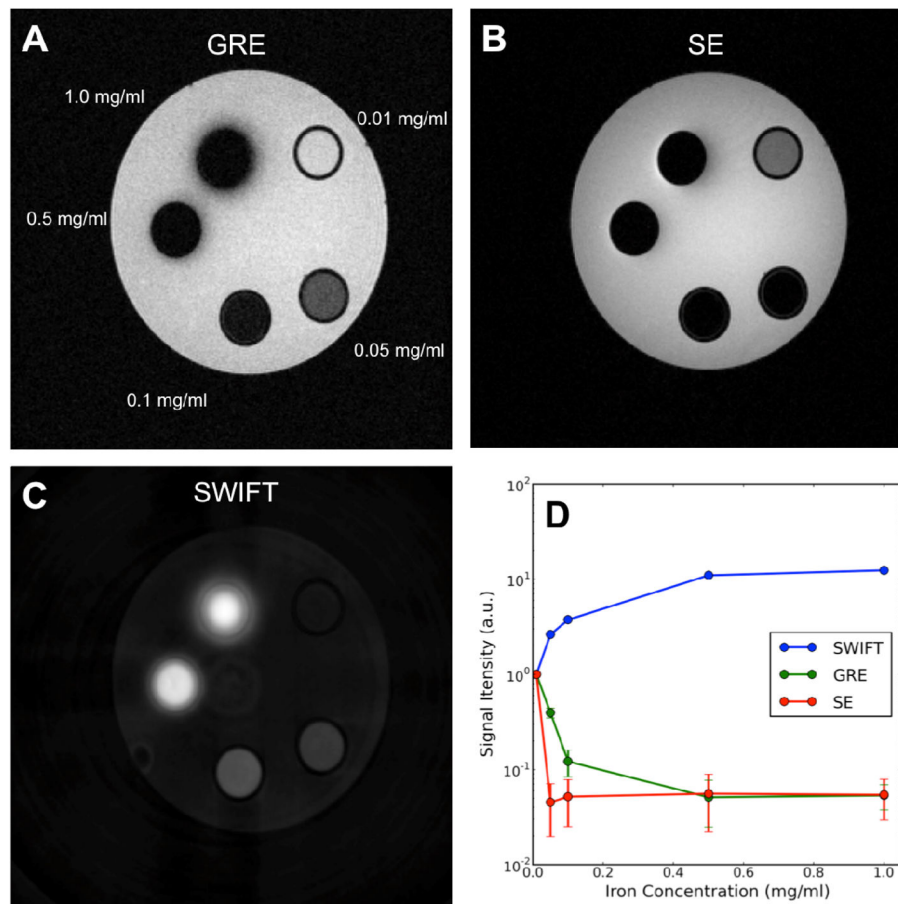


Figure 7. Positive contrast for super-paramagnetic iron-oxide nanoparticles using SWIFT. Shown are images of 5 tubes containing different concentrations of MNPs (Ferrotec (Santa Clara, CA 95054 USA) EMG-308; diameter ~10 nm) in 1% agarose gel, placed in a beaker of pure saline. Images were acquired with (A) GRE, (B) SE, and (C) SWIFT. With GRE and SE, there is a decrease in tube signal (the water signal in the tubes is normalized to the saline water signal in the beaker) with nanoparticle concentration, whereas with SWIFT the signal increases with concentration (D).

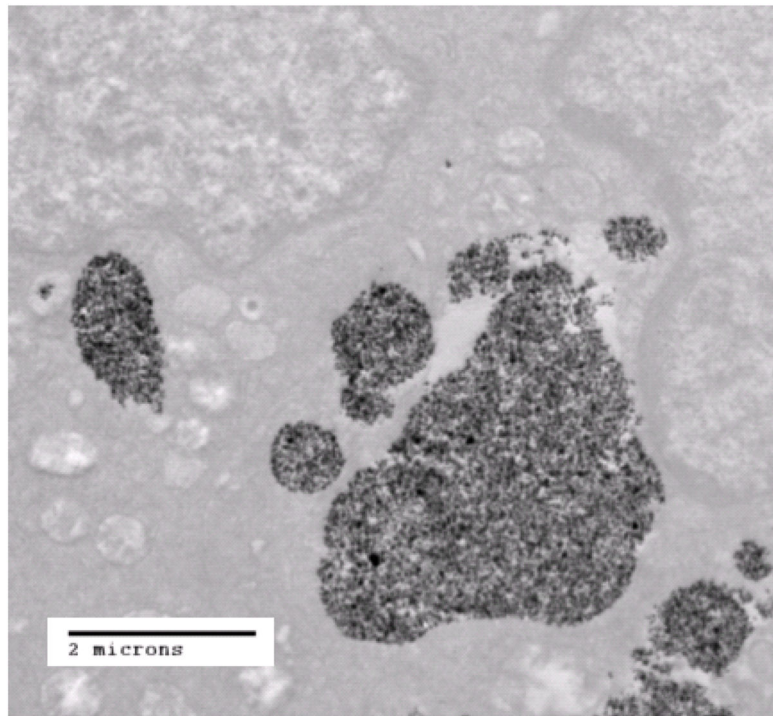


Figure 8.

Transmission electron micrograph of mouse mammary adenocarcinoma cells (*in vivo*) 3 hours post intra-tumoral delivery of 2.5 mg Fe/cc of tumor tissue (BNF IONPs, Micromod Partikeltechnologie GmbH (18119 Rostock-Warnemuende, GERMANY)). This study showed that all IONPs are either aggregated inside cells or had been eliminated from the tumor extracellular space after 24 hrs. The average size of the aggregates found is significantly larger than 200nm, the size at which SAR values dramatically increase.⁸ Such aggregation may also be detectable with SWIFT MRI.